Pergamon

Int. J. Solids Structures Vol. 35, No. 15, pp. 1709–1722, 1998

0020–7683/98 $19.00 + .00

PII: S0020–7683(97)00138–8

KINK BAND PROPAGATION AND BROADENING IN DUCTILE MATRIX FIBER COMPOSITES: EXPERIMENTS AND ANALYSIS

P. M. MORAN and C. F. SHIH
Division of Engineering, Brown University, Providence, Rhode Island 02912, U.S.A.

(*Received* 9 *April* 1996; *in revised form* 27 *November* 1996)

Abstract—Experimental observations of the kinking process in ductile matrix fiber composites confirm that kinking occurs in three distinct stages, incipient kinking, transient kinking and band broadening. Each of these stages is controlled by different kinematics. These stages and their underlying kinematics are described in detail in terms of soft deformation modes. New features revealed by our micrographs and experiments include: the tip of a propagating band lies at a shallower angle than the rest of the band, band broadening is steady-state phenomenon and occurs through localized micro-kink gliding. The experimentally measured steady-state band broadening stress is in agreement with a previous analytical prediction. © 1998 Elsevier Science Ltd.

1. INTRODUCTION

Kinking is the dominant compression failure mechanism in unidirectional fibre composites. Early research focussed on predicting the peak compressive strength [see for example Argon (1972); Chaplin (1977); Budiansky (1983)]. The first observations of kink band broadening in the post-peak stress regime were reported by Moran *et al.* (1995), see Fig. 1. Guided by their observations they separated kinking into three distinct stages characterized by different kinematics: incipient kinking, transient kinking and band broadening. This first study led them to predict that band broadening is a steady-state phenomenon (i.e. it occurs under a constant applied load). However, their experimental setup did not allow them to measure the loads associated with the different kinking stages. In the present work, experiments on ductile matrix fiber composites were conducted to measure the loads during kinking failure. These experiments confirm that band broadening is indeed a steady-state phenomenon, and that kinking may be separated into three distinct stages. Furthermore, our experiments reveal the detailed kinematics involved in kink band propagation. The new features of this work are:

- the tip of an advancing band lies at a shallower angle than the rest of the band;
- band broadening is steady-state phenomenon and occurs through localized micro-kink gliding;
- the steady-state stress has been measured.

The three stages of kinking are described individually below.

Incipient kinking is caused by imperfections such as localized regions of misaligned fibers. Shearing of the matrix between misaligned fibers allows for a soft mode of deformation during loading. The shearing and subsequent rotation of the fibers within these regions causes the load–displacement curve to become nonlinear, see Fig. 2. The regime between the onset of nonlinearity and the peak stress is referred to as incipient kinking.

After peak stress is attained, the stress drops dynamically until it reaches a steady-state value. During this stress drop, referred to as the transient kinking stage, a dominant kink band propagates across the specimen. As the band propagates the fibers within the tip of the kink band rotate. In order to accommodate this the tip of the kink band lies at a shallower angle than the rest of the band. During fiber rotation the matrix undergoes severe shear straining. Eventually, the matrix strain hardens to the point where further fiber rotation is not energetically favorable. At this point the fibers within the band become

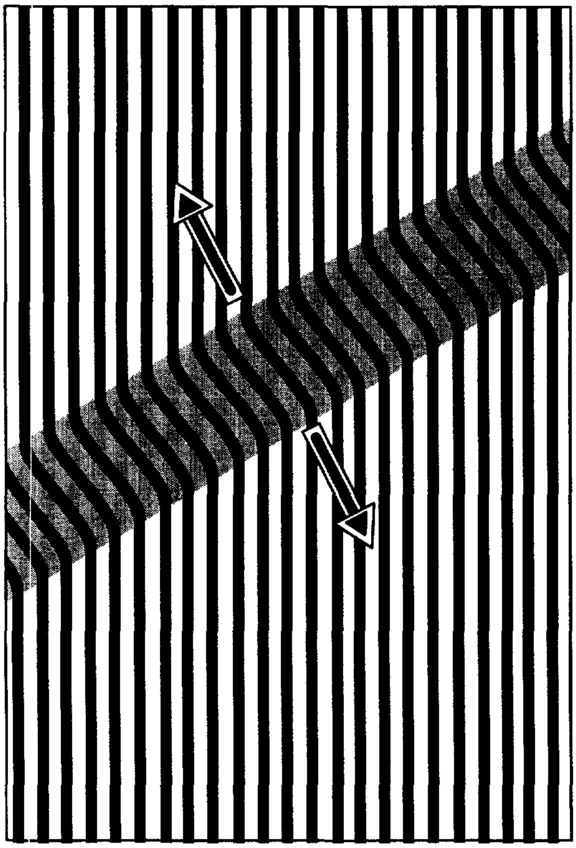

Fig. 1. Schematic of steady-state kink band broadening in which the edges propagate laterally into unhardened material. The material within the band is strain hardened and is highly resistant to further deformation [reproduced from Moran *et al.* (1995)].

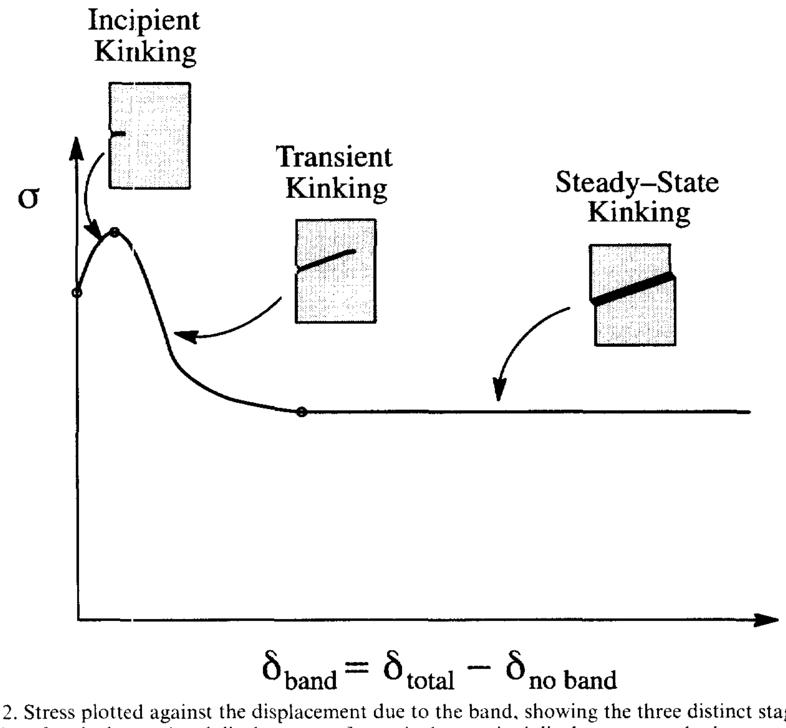

Fig. 2. Stress plotted against the displacement due to the band, showing the three distinct stages of kinking. δ_{total} is the total end displacement, $\delta_{no\ band}$ is the nominal displacement under homogeneous deformation (when the band is absent).

locked in their orientation, and a softer mode deformation is activated. This mode occurs a short distance behind the advancing tip. The new deformation mode involves broadening of the band by lateral propagation of its edges into softer (non-strain hardened) material. On a microscopic scale band broadening takes place by localized micro-kink gliding.

The key macroscopic features of band broadening are (see Fig. 1):

- within the band the fibers are locked at their final angle, as seen in post-mortem observations;
- the kink band orientation is fixed at its final angle;
- band broadening is a steady-state phenomenon and the driving stress is constant;
- the driving stress for band broadening is significantly lower than the peak stress and, unlike the peak stress, it is insensitive to material and geometric imperfections.

Throughout this paper we introduce and describe the mechanisms governing kinking in the context of the softest deformation modes. In the section which follows, we discuss the experimental setup and test results. Thereafter, the kinematics governing kinking are described. We present models for steady-state kinking, and for propagating kink bands in Section 4.

2. EXPERIMENTS

2.1. *Experimental setup*

We used the same type of specimens in this study as used by Moran *et al.* (1995). The specimen preparation and experimental setup was also very similar. The composites used in the experiments were ICI Fiberite APC-2. This unidirectional fiber composite consists of a Victrex PEEK matrix with 60% volume fraction of IM7 carbon fibers. The specimens were roughly 45 mm in length and had a 10 mm by 6 mm rectangular cross-section. A notch of between 1.5 and 2 mm in length was cut leaving a ligament roughly 4 or 4.5 mm long and 10 mm wide ahead of the notch. A cross-section of a typical notch is shown in Fig. 3. To properly record steady-state kinking, the notch must have the following characteristics:

(1) It must be deep enough to ensure the kink band will initiate from it.
(2) Its sides must be far enough apart so as not to close onto each other during deformation.
(3) Its sides must interfere with the end of the broadening band as little as possible.

The notches were made by making five parallel cuts with a diamond saw. The center cut was made slightly deeper than the rest. The ends of the four even lengthed cuts were filed flat. The end of the center cut was sharpened with a razorblade.

The specimen was clamped on the sides to allow only in-plane deformation to occur. The clamping rig was made from steel plates. The front plate had a thick glass window in it so the progression of the kink band could be observed. A rubber gasket was positioned between the glass window and the steel plate to accommodate slight specimen/fixture misalignments. A thin film of oil was kept between the clamping rig and specimen to minimize friction and promote plane strain conditions. This clamping rig is the same as that used by Moran *et al.* (1995), a picture of it can be seen in Fig. 4. An Instron 4505 machine was used to apply displacement controlled loading to the specimen in the fiber direction. The displacement velocity was 0.05 mm/min. The kink band was monitored during loading and a load–displacement record was kept.

The friction between the clamping rig and the specimen was measured by pushing a clamped specimen through the rig. The force needed to push the specimen was roughly 125 newtons. This is two orders of magnitude lower than the forces applied during testing and, therefore, we are satisfied that the effects of friction between the clamping rig and the specimen are negligible.

The specimen was loaded between two flat plates in the Instron machine. The friction between the loading plates and the ends of the specimen inhibits the lateral motion of the specimen ends. As a result a shear stress and a bending moment may arise in the specimen.

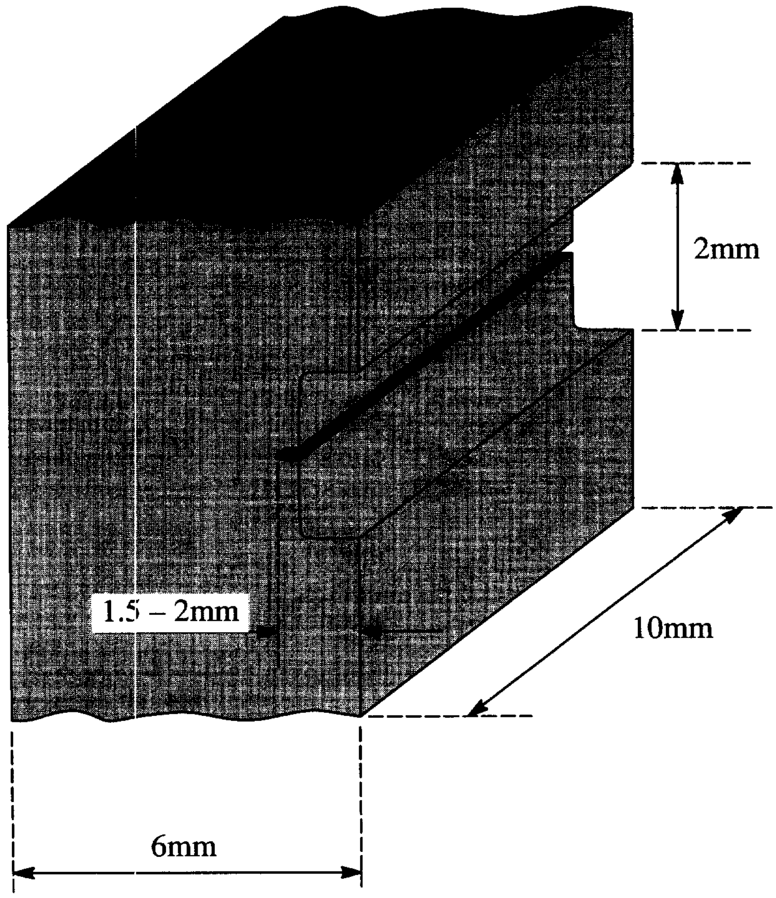

Fig. 3. Typical cross-section of a notched specimen.

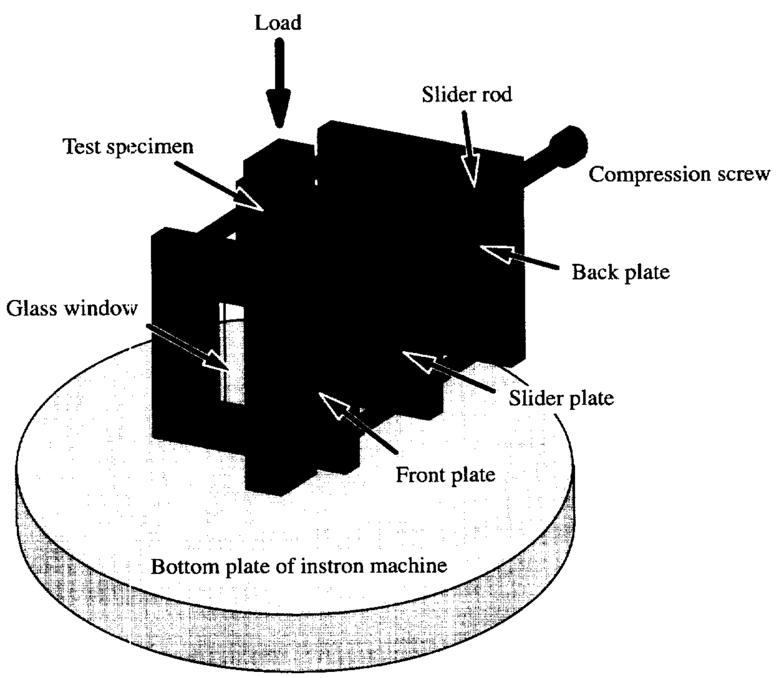

Fig. 4. Clamping rig used in experiments to impose plan strain conditions [reproduced from Moran *et al.* (1995)].

However, the specimen is long when compared with both the ligament length and the kink band width and we believe that these stresses do not affect the results significantly.

2.2. *Experimental observations*

Figure 5 shows typical experimental load–displacement curves. The specimens are relatively stiff and a portion of the displacements shown are due to machine offset and compliance. It is difficult to accurately subtract machine offset from the data. Since the critical features of our observations are independent of the exact machine displacements, we do not attempt to subtract machine settling and compliance from our data, but rather choose to present the raw data.

Initially the deformation is linear elastic. Incipient kinking occurs shortly before the peak load is attained and causes a nonlinearity in the load–displacement curve. Because typical carbon fiber composites are stiff and relatively free of defects, the nonlinearity is often difficult to see. However, careful observation of each of the curves reveals some nonlinearity just prior to peak stress. In materials which are softer and contain more defects it is easier to observe incipient kinking [see Poulsen *et al.* (1997)]. For our specimens we have measured peak stresses ranging between 440 and 660 MPa. In the transient kinking region the load drops sharply from the peak load to the steady-state load. Transient kinking is not captured in detail in these experiments since it is dynamic and is too fast for our machine to record. After transient kinking the specimen reaches the steady-state band broadening stage which is stable and can be seen clearly on the load–displacement curves. The steady-state stresses lie between 300 and 350 MPa. The loading was terminated when the kink band width reached between 250 and 500 μm or when the load dropped below steady-state.

The present experiments show a constant post critical steady-state broadening load, confirming the predictions made by Moran *et al.* (1995). The scatter in the steady-state data is small. The stress needed to drive steady-state band broadening is measured to be roughly five times the shear yield stress of the composite. Video recordings show that during steady-state loading the band broadens substantially while both the fibers within the kink band and the kink band itself remain fixed in their orientation. The width of the kink band after broadening may be of the order of 100 fiber diameters. Careful observations of band broadening band reveal a localized micro-kink gliding along the edges of the kink band in the manner shown in Fig. 6. This is similar to dislocation-kink gliding seen in dislocation studies. Ahead of the micro-kink the band has a width of 'W'. Behind the micro-kink the

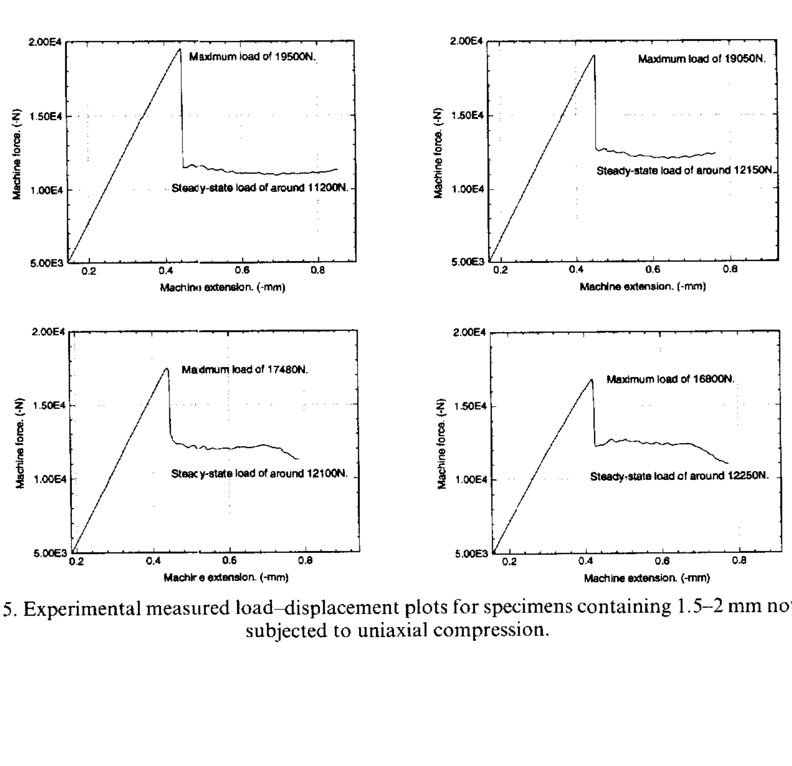

Fig. 5. Experimental measured load–displacement plots for specimens containing 1.5–2 mm notches subjected to uniaxial compression.

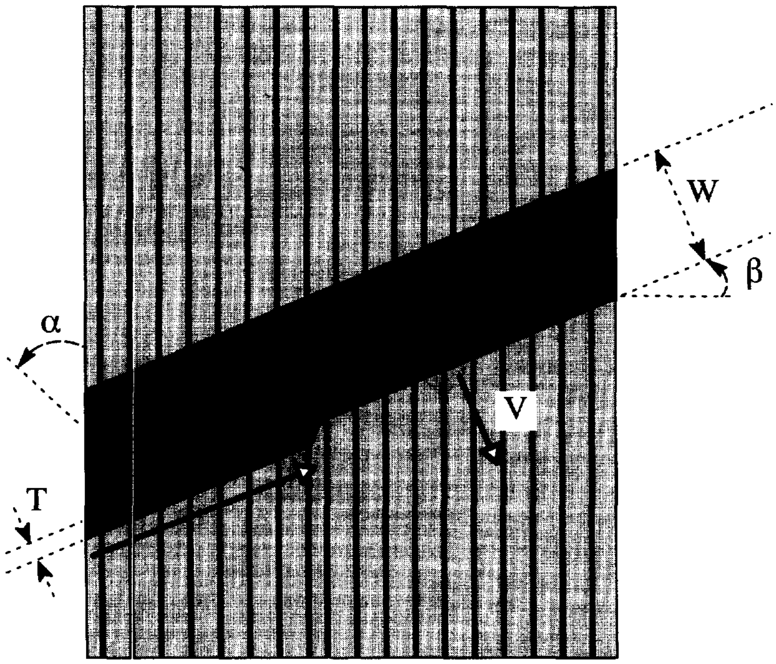

Fig. 6. A localized micro-kink gliding transversely along the band resulting in overall band broadening at a velocity V.

band has been broadened to a width of '$W+T$', where 'T' is the thickness of the micro-kink. These micro-kinks appear to initiate from an imperfection such as the notch or specimen boundary, and then run rapidly across the specimen.

After band broadening some specimens were unloaded and the material above the top edge of the kink was cut away. This leaves the highly deformed material within the kink band unsupported from the top. No break-up of the material was observed, and the curved fibers within the band did not straighten. This supports the argument that the matrix within the kink band undergoes severe plastic straining, and that debonding between the matrix and fibers is not significant.

In additional experiments we increased the notch length to 3–4 mm and recorded peak stresses as low as 390 MPa. This peak stress is roughly 50 MPa higher than the steady-state broadening stress for this material. In these specimens the nonlinearity due to incipient kinking is far more pronounced. In some of these experiments we were able to video record a kink band propagating during the incipient and transient stages. The tip of a propagating kink band appears to be bent, i.e. the tip lies at a shallower angle than the rest of the band, see Fig. 7; a schematic is shown in Fig. 8. The clamping rig shown in Fig. 4 was used to impose plane strain conditions on the specimens during the experiments. The specimens were illuminated from one side only. As a result the fibers reflected different amounts of light depending on their orientation with respect to the light source. This allows us to see the kink band easily. Figure 7(a) shows a kink band during incipient kinking. The fibers can be seen running vertically from the top to the bottom of the picture. The notch is on the right-hand side of the figure. The thin dark line extending upwards to the left of the notch is the kink band. The kink band lies at a shallow angle and the fibers within it are in the process of rotating. Figure 7(b) shows the kink band at a later stage of development. The white line drawn across the picture in Figs. 7(b, c) allow us to see the angle at which the kink band is propagating. Notice that the tip of the kink band appears to be bent. In the tip region the fibers have not rotated very far from their original positions and appear darker than their surroundings. At the base of the kink band (behind the tip) the fibers have reached their lock-up orientation. The light source is positioned so that the fibers reflect the maximum amount of light when they reach their lock-up orientation, and as a result this section of the kink band appears almost white in the figure. Figure 7(c) shows

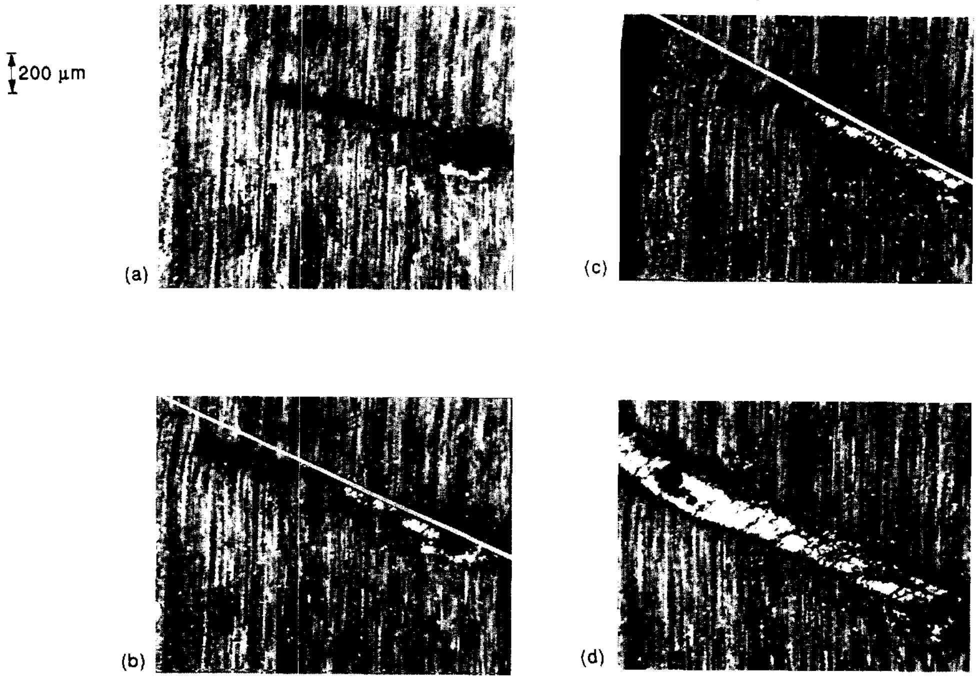

Fig. 7. Four *in situ* micrographs (obtained by video camera and ordered in sequence) showing kink band propagation and broadening.

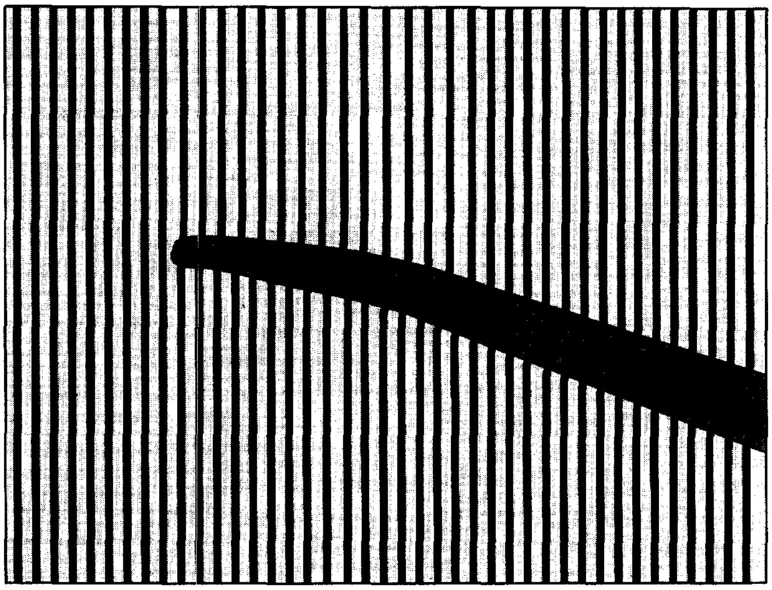

Fig. 8. Schematic snapshot of a kink band. The band is propagating from right to left in a ductile matrix fiber composite. The tip region lies at a shallower angle relative to the rest of the band. Observe that the fibres behind the tip region have stopped rotating while those in the tip region have rotated less and are still in the process of rotating.

the kink band after it has grown almost completely across the specimen. As in Fig. 7(a,b) the tip of the kink band lies at a shallower angle than the rest of the band. Just as before, the fibers in the tip region appear darker than the surrounding material because they are just beginning to rotate. The majority of the kink band appears white indicating that most of the fibers behind the tip of the band have locked-up. The final figure in the sequence shows a kink band which has propagated across the entire specimen and has broadened significantly. All the fibers within the band are locked in their final orientation, and the band is well defined by dark edges where the fibers are either severely bent or broken. Now the entire kink band lies at the same orientation and broadens laterally as further end-displacement is applied to the specimen. The section which follows offers an explanation for the features observed in the experiments.

3. DISCUSSION OF KINEMATICS

Incipient kinking, transient kinking and steady-state kinking are discussed separately. We assume that the ductile matrix is essentially volume preserving, and the fibres are inextensible. These assumptions are valid for carbon fiber PEEK composites, the material under study. Given these assumptions, Chaplin (1977) argued that the kink band angle, β, must be related to the angle through which the fibers have rotated, α, in the following way

$$\beta = \frac{\alpha}{2} \tag{1}$$

due to compatibility; α and β are defined in Fig. 6. We use relation (1) to provide an explanation for some of our observations.

3.1. *Incipient kinking*

Consider a uniaxial fiber composite specimen with vertically aligned fibers. The specimen contains a localized region of misaligned fibers. The specimen is loaded in the fiber direction. Initially the loading is linear elastic. As the load increases the resolved shear stress acting on the matrix between the misaligned fibers increases too. Eventually the matrix yields plastically. This causes the load curve to exhibit some nonlinearity, and marks the beginning of the incipient kinking stage, see Fig. 2. The easiest mode of deformation during this stage is for the misaligned fibers within the localized area to buckle and rotate away from their initial vertical orientation. As these fibers rotate, both the resolved shear stress on the matrix, and the bending moment on the fibers increase. This localized geometric softening of the material causes nearby fibers to buckle, and eventually a small incipient kink band is formed.

The fibers within the kink band are rotated away from the vertical by a small amount, i.e. α is small. A consequence of volume preservation is that a small α implies a small β, see eqn (1). Therefore, the limited fiber rotation at early kinking dictates a shallow kink band angle. However, as the fibers rotate the band itself must rotate in order to maintain relation (1). Support for this can be found from both experimental and finite element studies. The incipient kink band shown in Fig. 7(a) lies at a shallower angle than it does in later stages, see Fig. 7(b–d). A shallow rotating kink band can also be seen in the experimental micrographs presented by Moran *et al.* (1995). The finite element analysis performed by Kyriakides *et al.* (1995) also clearly shows a small kink band forming at a shallow angle and rotating to a steep angle. Fleck and Shu (1996) also conducted a finite element study of kinking. Their calculations show that the initial kink band always formed at a shallow angle regardless of the initial imperfection orientation. The above studies taken together provide clear evidence that kink bands form at a shallow angle and must rotate to a steeper angle as kinking progresses.

Typically the concomitant kink band and fiber rotation characteristic of incipient kinking occurs stably for only a short time before the peak load is attained. In fact in carbon fiber composites incipient kinking often begins so close to the peak load that the nonlinearity it causes is only barely noticeable. Peak load marks the end of the incipient kinking stage. Most research thus far has dealt with the prediction of the peak stress [Argon (1972); Chaplin (1977); Budiansky (1983); Budiansky and Fleck (1993); Fleck and Shu (1996)].

3.2. *Transient kinking*

After the peak load is attained, the load drops dynamically, see Fig. 5. This is called the transient kinking stage. Little is known about the transient stage due to its unstable nature. In some of our experiments, however, we were able to observe kink bands propagating stably in the transient stage, see Fig. 7. In these experiments the notch lengths were very long, and some of the observed features may be accentuated by notch effects. Nevertheless, we believe that the observed features are characteristic of a kink band propagating through a thick body. A schematic of a propagating kink band is shown in Fig. 8. Here the tip of the band is depicted as a well defined narrow region. In reality, however, the tip of the band is difficult to define precisely, and the wavelength of the rotating fibers may be fairly long. What is evident from Fig. 7 is that the plastic deformation localizes within a narrow bent tip as shown in Fig. 8. Two key features can be clearly seen from the figures:

- in the tip region the fibers rotate and the kink band itself changes orientation
- behind the tip region there is no further rotation of the band or the fibers.

These features can be explained with the help of eqn (1) and the fact that the matrix is a ductile strain hardening material. It follows from eqn (1) that any rotation of the fibers must be accompanied by a rotation of the kink band itself, i.e. it is the fiber rotation which drives the band to rotate, as is seen in the tip region. During fiber rotation the matrix undergoes significant shear straining. This shear strain hardening stiffens the response of the material within the band. Eventually the material is strain hardened to the point that the fibers stop rotating. Thereafter, the fibers are locked in their final orientation and consequently so is the band. Therefore, we believe it is the shear strain hardening of the material which dictates the fiber lock-up orientation and the final kink band angle.

After fiber lock-up the easiest mode of deformation is for the band to broaden laterally into the surrounding material, which has not yet undergone strain hardening. This can be seen behind the tip region in Fig. 8, and is discussed further in the section which follows.

3.3. *Steady-state kinking*

Once the kink band has propagated across the entire specimen, the load stabilizes at a level below the peak load, see Fig. 5. This marks the beginning of the steady-state band broadening. During this stage we observe the entire kink band broadening under a constant applied load. Band broadening occurs by a outward propagation of the band edges while the fibers within the band and the band itself remain at fixed orientations.

Our explanation for band broadening is as follows. The material within the band is highly deformed and strain hardened. In contrast the material outside the band is plastically unstrained and is easily sheared. Band broadening into this material provides a soft alternative mechanism to accommodate further remote deformation.

On the microscopic scale band broadening need not occur uniformly along the band edges. A micromechanism of kink band broadening is shown in Fig. 6. This mechanism, which we call 'localized micro-kink gliding', is similar to 'dislocation-kink gliding' seen at dislocation fronts. It is well known that dislocation fronts do not advance uniformly. Instead a dislocation-kink, typically a lattice spacing wide, glides transversely across the front resulting in dislocation advance. This is clearly the easiest way to advance a dislocation. The situation is similar for broadening kink bands. Instead of the entire band edge advancing uniformly, a portion of it advances while the rest of it remains stationary. This results in a localized micro-kink gliding transversely along the length of the kink band, see Fig. 6. These micro-kinks propagate rapidly across the specimen broadening the band as they advance. They are on the order of a fiber diameter wide. Given micro-kink width, T, a relationship exists between the kink band broadening velocity, V, and the rate of initiation of micro-kinks, R:

$$V = RT. \tag{2}$$

The velocity of the micro-kinks is much greater than V. Since V is related to the specimen end-shortening velocity $\dot{\delta}$, we may write the initiation rate, R, as

$$R = \frac{\dot{\delta}\cos\beta}{2T\sin^2\beta} \tag{3}$$

where β is the kink band angle. Equation (3) shows that the micro-kink initiation rate is directly proportional to the rate of applied displacement $\dot{\delta}$. The above micromechanics analysis warrants further study, but will not be discussed further here.

For the purpose of computing the steady-state band broadening stress it is sufficient to assume that the band edges advance uniformly. This is discussed in the section which follows.

4. KINK BAND MODELING

4.1. *Infinite band model for steady-state kinking*

Moran *et al.* (1995) proposed a simple one-dimensional model to derive steady-state kinking stress. They used energy arguments, and assumed an infinite kink band broadening uniformly along its length in order to obtain an explicit relation between the steady-state kinking stress, σ_{ss}, and the relevant material and geometric parameters. We emphasize that this result is independent of whether the kink band broadens uniformly or by localized micro-kink gliding. The analysis also assumes that the fibres do not break during broadening and the energy dissipation arises solely from the plastic deformation of the matrix. The energy dissipated by brittle fiber fracture is clearly a second-order when compared to matrix plastic dissipation. Thus, it does not affect the steady-state stress, σ_{ss}. Fibers breaking during band broadening have recently been observed by Sivashanker *et al.* (1997), and Vogler and Kyriakides (1997).

Moran *et al.* (1995) assumed a piece-wise linear approximation to the composite's shear stress–strain relation, based on tests performed by Arruda and Boyce (1993), and Dahoun *et al.* (1993, 1995). Using this approximation they found a relation for the applied stress required to drive band broadening, σ_{ss}:

$$\sigma_{ss} = \frac{1}{2\sin^2\beta}\left[\tau_y\left(2\tan\beta - \frac{\gamma_y}{2}\right) + \frac{1}{2}G_s(2\tan\beta - \gamma_s)^2\right]. \tag{4}$$

Here τ_y is the shear yield stress of the composite. γ_y is the composite's shear yield strain. γ_s is the shear strain after which linear hardening is assumed to occur. G_s is the shear modulus associated with the linear hardening.

Using eqn (4) and making an argument that the energetically favorable mode is the solution to the problem, they obtained an expression for the kink band angle, β:

$$\tau_y\left(\tan^3\beta - \tan\beta + \frac{\gamma_y}{2}\right) + G_s(2\tan\beta - \gamma_s)\left(\tan^3\beta + \frac{\gamma_s}{2}\right) = 0. \tag{5}$$

The kink band angle for ductile polymer matrix composites was predicted to lie between 10 and 35°, depending on the shear properties of the composite. The corresponding steady-state driving stress was predicted to be between 3 and 7 times the shear yield stress of the composite.

Our experiments (see Fig. 5) confirm that band broadening is indeed a steady-state phenomenon. We measured the kink band angle to be about 22° and the steady-state broadening stress to be approximately five times the composite's shear yield stress. Both measurements show agreement with eqns (4) and (5).

4.2. *Kink band propagation model*

A fracture mechanics approach may be employed to model propagating kink bands. The kink band may be thought of as a mode II dominant crack propagating in an anisotropic material. The crack supports bridging stresses along its length. A large fraction of the

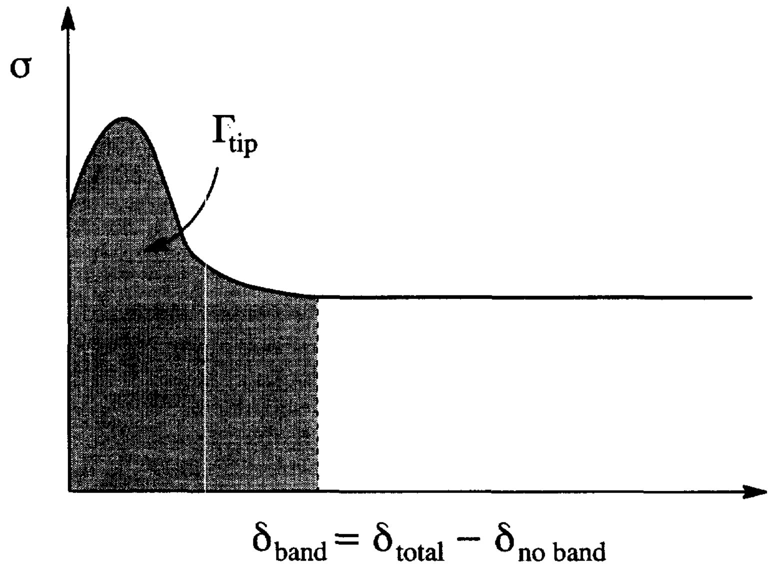

Fig. 9. A plot showing applied stress vs displacement due to the band. The shaded area is Γ_{tip} arising from the dissipative processes in the tip region.

propagating kink band (behind the tip) undergoes band broadening. Therefore the bridging stress in this region is given by eqn (5). This applied stress has been measured in this paper and by Vogler and Kyriakides (1997).

The kinematics and geometry of the kink band tip are complicated, and predicting the bridging stresses in this region poses a greater challenge. Nevertheless, there are several ways of doing this, and some are listed below.

(1) Certain simplifying assumptions may be made to obtain an analytical solution for the bridging stresses in the tip region [see Liu and Shih (1996)].
(2) A relation for the stress versus the displacement *due to the kink band* (Fig. 9) may be constructed using an experimental stress versus end shortening displacement curve. The shaded region in Fig. 9 is the energy taken to initiate a kink band. This represents the energy taken to bend the fibers, plus the initial elastic and plastic shearing on the matrix, up to the point of fiber lock-up. Since the same processes occur in the tip of a propagating band, it is reasonable to assume that the tip toughness is also given by the shaded region of Fig. 9. Using these arguments it is possible to use the approach outlined by Gu (1993) to analyze propagating bands.
(3) The strains around a propagating kink band tip may be measured directly by Moire methods. The bridging stresses may be calculated from the strain field.

5. DESIGNING WITH ALIGNED FIBER COMPOSITES

5.1. *Peak stress and steady-state stress*

Liu *et al.* (1996) discussed two design approaches, one based on the peak stress, and the other based on the steady-state band broadening stress. Although we will not present these two approaches in detail here, the concepts behind them are summarized below.

By using peak stress as the design parameter one is able to fully utilize the strength of the composite. However, it is well known that peak stress is highly imperfection sensitive and knock-down factors must be applied. Furthermore, the structure needs to be carefully inspected both prior to installation and during service to insure that defects are not introduced.

Steady-state stress on the other hand is not sensitive to either geometric or material imperfections. It provides a lower bound to the peak stress. This makes it both easier and safer to design with, especially when defects such as holes or joints are introduced into the structure. The disadvantage of this design approach is that the full strength of the composite is not utilized.

A third design approach, the damage tolerance approach, is useful in large structures such as ships or submarines where it is both costly and impractical to routinely change structural components. In these applications it is vital that the components be able to withstand a limited amount of damage without failing. A simple method for assessing the damage tolerance of a component is proposed below.

5.2. *Damage tolerance*

Consider a large composite structure containing a small kink band, see Fig. 11. We can divide the structure into three regions; the good region ahead of the kink band, the tip of the kink band, and the region behind the tip of the kink band. Ahead of the kink band the material is undamaged. Therefore, this region is still able to support stresses up to the material's theoretical peak stress, σ_p. The tip region is able to support stresses between the peak stress and the steady-state band broadening stress. Behind the tip the kink band broadens and is able to support stresses up to the steady-state band broadening stress, σ_{ss}. Since the tip region is usually very small when compared with either of the other two regions it can be neglected. Therefore, the remotely applied stress needed to propagate the kink band, σ_r, can be estimated by

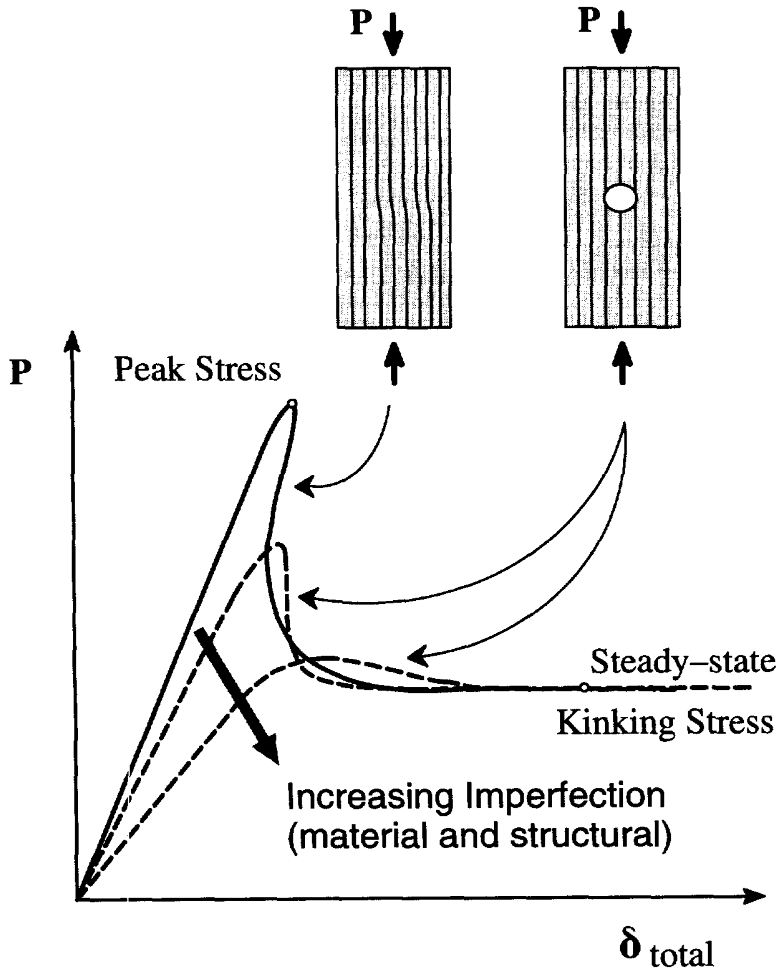

Fig. 10. Schematic compressive stress–displacement curves showing the effect of imperfections on peak stress and post-peak stress behavior for geometries with nominally identical cross-sections [reproduced from Liu *et al.* (1996)].

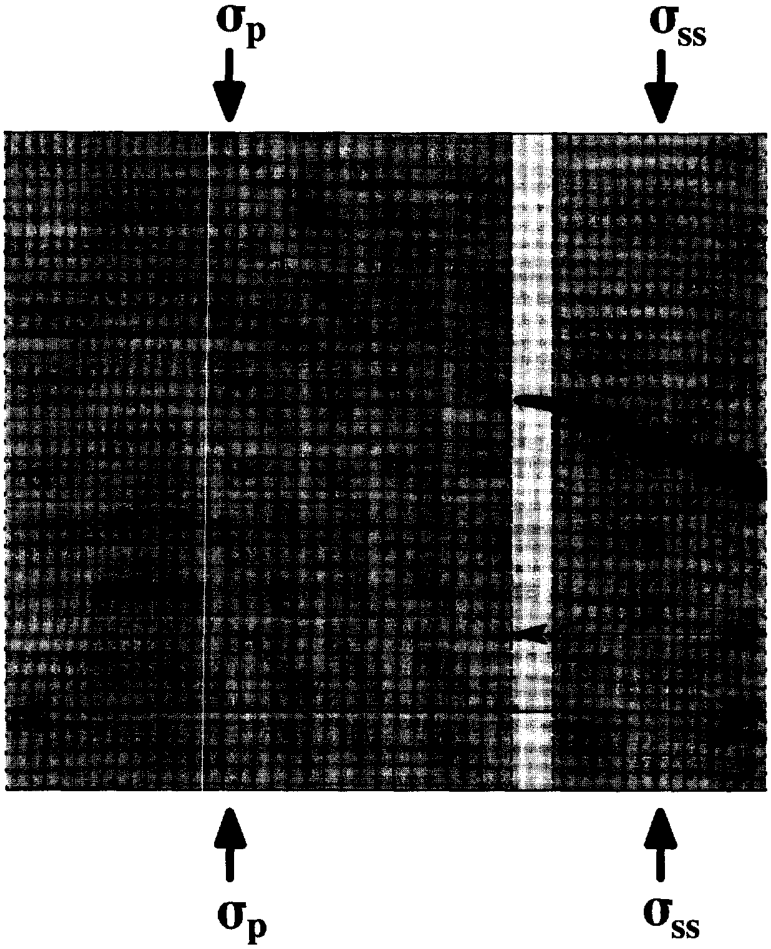

Fig. 11. Kink band propagating from right to left in an aligned fiber composite. The region undergoing band broadening can support the steady-state stress, σ_{ss}. The material ahead of the kink band is able to support the peak stress, σ_p.

$$\sigma_r \approx \frac{L\sigma_{ss} + (W-L)\sigma_p}{W} \tag{6}$$

where L is the length of the kink band, and W is the width of the composite structure, see Fig. 11. Result (6) may be applied as an engineering damage tolerance model.

6. DISCUSSION

The newly observed features pertaining to kink band propagation and steady-state band broadening presented in this paper are:

- we observe that the tip of a propagating band lies at a shallower angle than the rest of the band;
- we confirm experimentally that band broadening is steady-state phenomenon and find that it occurs through localized micro-kink gliding;
- we have measured the steady-state stress.

How a kink band propagates across a specimen is an issue that has been largely unresolved. Our observations provide an explanation for this process. We observe kink bands which are shallower at their tip than throughout the rest ot the band, see Figs 7 and 8. Within the tip region of a propagating band the fibers rotate from their undeformed position to their final lock-up orientation. The band's tip region steepens its orientation to allow this fiber rotation without violating eqn (1). Behind the tip region the band is macroscopically straight; here the fibers are locked-up and no further deformation occurs within the band. However, the band is able to broaden laterally by the outward propagation of its edges into the unhardened material surrounding it. Our experiments show bands broadening under a constant applied stress of about five times the shear yield stress of the composite. This is in agreement with Moran *et al.* who predicted band broadening to be a steady-state phenomenon occurring at an applied load of 3–7 times the composite's shear yield stress.

The edges of a broadening band have been observed on a microscopic scale. The band edges do not necessarily propagate outwards uniformly. Instead we have observed that broadening occurs by micro-kinks gliding tangentially along the band edges, see Fig. 6. Micro-kink gliding provides an easy band broadening mechanism. This mechanism is similar to a dislocation–kink, typically a lattice spacing wide, gliding transversely across the dislocation front.

The three stages of kinking are identifiable from Figs 5 and 7. Three different design philosophies making use of the peak and steady-state stresses are discussed. Designing with the peak stress utilizes the full strength of the composite. However, the peak stress is highly sensitive to imperfections and they must be controlled and carefully monitored. Designing with the steady-state band broadening stress has the disadvantage of being overly conservative in some situations. However, the steady-state stress is unaffected by both material and geometric imperfections and provides a lower bound design approach. A damage tolerance approach is useful in large structures which are expected to withstand some damage while in service. In this situation the steady-state stress can be too conservative while the peak stress is overly optimistic. The damage tolerance model proposed here provides a straightforward method for assessing the strength of a structure.

Acknowledgements—This investigation is supported by the Office of Naval Research through Grant N00014-95-1-0399 and the National Science Foundation under the Materials Research Group Grant no. DMR-9223683. We are grateful to Professor R. J. Clifton for helpful discussions, and to Professor K.-S. Kim for the use of his experimental facilities.

REFERENCES

Argon, A. S. (1972) Fracture of composites. In *Treatise of Materials Science and Technology*, ed. H. Herman, Vol. 1 pp. 79–114. Academic Press, New York.

Arruda, E. M. and Boyce, M. C. (1993) Evolution of plastic anisotropy in amorphous polymers during finite straining. *International Journal of Plasticity* **9**, 697.

Budiansky, B. (1983) Micromechanics. *Computers and Structures* **16**, 3–12.

Budiansky, B. and Fleck, N. A. (1993) Compressive failure of fibre composites. *Journal of Mechanics and Physics of Solids* **41**, 183–211.

Chaplin, C. R. (1977) Compressive fracture in unidirectional glass-reinforced plastics. *Journal of Material Science* **12**, 347–352.

Dahoun, A., G'Sell, C., Molinari, A. and Canova, G. R. (1993) Plastic behavior and deformation textures of poly(ether ether ketone) under uniaxial tension and simple shear. *ASME MD-Vol.* **46**, 57–76.

Dahoun, A., Aboulfaraj, M., G'Sell, C., Molinari, A. and Canova, G. R. (1995) Plastic behavior and deformation textures of poly(ether ether ketone) under uniaxial tension and simple shear. *Polymer Engineering Science* **35**, 317.

Fleck, N. A. and Shu, J. Y. (1996) Microbuckle initiation in fibre composites: a finite element study. *Journal of Mechanics and Physics of Solids* **43**(12), 1887–1918.

Gu, P. (1993) PhD thesis, Brown University.

Kyriakides, S., Arseculeratne, R., Perry, E. J. and Liechti, K. M. (1995) On the compressive failure of fiber reinforced composites. *International Journal of Solids and Structures* **32**, 689–738.

Liu, X. H., Moran, P. M. and Shih, C. F. (1996) The mechanics of compressive kinking in unidirectional fiber reinforced ductile matrix composites. *Composites Engineering* Part B, **27B**, 553–560.

Liu, X. H. and Shih, C. F. (1996) Micromechanics of compressive kinking in composites. *Acta Metallica Material* (submitted).

Moran, P. M., Liu, X. H. and Shih, C. F. (1995) Kink band formation and band broadening in fiber composites under compressive loading. *Acta Metallica Material* **43**, 2943–2958.

Poulsen, J. S., Moran, P. M., Shih, C. F. and Byskov, E. (1997) Kink band initiation and band broadening in clear wood under compressive loading. *Mechanics of Materials* **25**, 67–77.

Sivashanker, S., Fleck, N. A. and Sutcliffe, M. P. F. (1997) Microbuckle propagation in a unidirectional carbon fibre–epoxy matrix composite. *Acta Metallica Material* **42**(7), 2219–2231.

Vogler, T. J. and Kyriakides, S. (1997) Initiation and axial propagation of kink bands in fiber composites. *Acta Metallica Material* **45**(6), 2443–2454.